

# Far from resolved: Stromal cell-based iTRAQ research of muscle-invasive bladder cancer regarding heterogeneity

PENG-FEI LIU<sup>1,2\*</sup>, YONG-HUA WANG<sup>1\*</sup>, YAN-WEI CAO<sup>1,3</sup>, HAI-PING JIANG<sup>4</sup>, XUE-CHENG YANG<sup>1</sup>,  
XIN-SHENG WANG<sup>1</sup> and HAI-TAO NIU<sup>1,3</sup>

<sup>1</sup>Department of Urology, The Affiliated Hospital of Qingdao University, Qingdao 266101; <sup>2</sup>The Medical College of Qingdao University, Qingdao 266071; <sup>3</sup>Key Urology Laboratory of Qingdao City, Qingdao 266101;

<sup>4</sup>Department of Oncology, The Affiliated Hospital of Qingdao University, Qingdao 266101, P.R. China

Received May 2, 2014; Accepted July 4, 2014

DOI: 10.3892/or.2014.3340

**Abstract.** The aim of the present study was to globally characterize the cancer stroma expression profile of muscle-invasive bladder cancer in different metastatic risk groups and to discuss the decisive role of biological pathway change in cancer heterogeneity. Laser capture microdissection was employed to harvest purified muscle-invasive bladder cancer stromal cells derived from 30 clinical samples deriving from 3 different metastatic risk groups. Isobaric tags for relative and absolute quantitation (iTRAQ) and two-dimensional liquid chromatography tandem mass spectrometry (2D LC-MS/MS) were used to identify the differentially expressed proteins. Subsequently, the differentially expressed proteins were further analyzed by bioinformatics tools. After completing the above tasks, the proteins of interest were further compared with the published literature. We identified 1,049 differentially expressed proteins by paired comparison (high risk vs. median, low risk and normal groups; median risk vs. low risk and normal groups, low risk vs. normal group; a total of 6 comparisons). A total of 510,549,548 proteins as significantly altered (ratio fold-change  $\geq 1.5$  or  $\leq 0.667$  between the metastatic potential risk group and the normal group) were presented in the low/median/high metastatic risk group, respectively. Pathway analysis revealed that the differentially expressed proteins were mainly located in the Kyoto Encyclopedia of Genes and Genomes pathways, including focal adhesion pathway, systemic lupus erythematosus pathway and ECM-receptor interaction pathway. In addition, several proteins such as EXOC4, MYH10 and MMP-9 may serve as candidate biomarkers of muscle-invasive bladder cancer. Our study

confirmed that stromal cells, an important part of the cancer tissue, are pivotal for regulating the heterogeneity of cancer. Common changes in biological pathways determined the malignant phenotype of muscle-invasive bladder cancer, and biomarker discovery should take into account both neoplastic cells and their corresponding stromata.

## Introduction

Bladder cancer is one of the most common urologic malignant disease and shows an increasing tendency worldwide (1). Tremendous difference in prognosis is noted among patients with muscle-invasive bladder cancer under the same condition of pathological stage and grade (2). Therefore, heterogeneity plays a crucial role in the metastatic potential risk for muscle-invasive bladder cancer patients. In recent decades, even though much research based on bladder cancer has been performed, the biological basis of this disease remains enigmatic (3). Our research based on proteomics is one way to explore the carcinogenic mechanism. In the present study, we performed quantitative research on muscle-invasive bladder cancer. The isobaric tag for relative and quantitation (iTRAQ) technique was employed to quantitatively analyze the protein expression levels of samples while covering the shortage of the traditional shot-gun strategy. The quantitative analysis of proteins also contributes to bladder cancer biomarker panel findings.

In recent years, the vital role of cancer stroma in metastatic potential heterogeneity has been the focus of cancer research (4). Research indicates that the dynamic changes in the extracellular matrix and changes in stromal biology signaling cascades are correlated with tumor metastatic potential (5). Tumor heterogeneity is influenced by several factors, such as the genetic contribution, cancer stem cell differentiation and the tumor microenvironment interaction. Regarding the tumor microenvironment, several types of non-neoplastic cells, such as cancer-associated fibroblasts, endothelial cells and immune cells, together constitute the tumor stroma and influence the heterogeneity of the tumor in various ways. Tumor heterogeneity can also be affected by bioactive proteins, such as immune and inflammatory factors (6). Due to changes in bioactive proteins, the biological pathway is altered correspondingly and reflects the features of heterogeneity in the

---

*Correspondence to:* Dr Hai-Tao Niu or Dr Xin-Sheng Wang, Department of Urology, The Affiliated Hospital of Qingdao University, 59 Haier Road, Laoshan, Qingdao 266101, P.R. China  
E-mail: niuht0532@126.com  
E-mail: wangxs0532@126.com

\*Contributed equally

**Key words:** muscle-invasive bladder cancer, stroma, biomarker panel, pathway, heterogeneity, proteomics

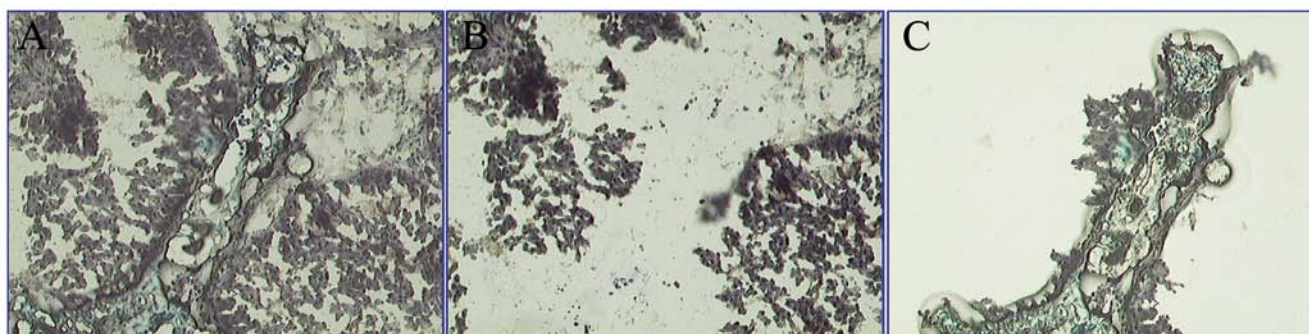


Figure 1. Harvesting of the cancer stroma by LCM. (A) Before and (B) after LCM. (C) The microdissected stromal cells on the cap.

tumor. In the present study, we aimed to explore the muscle-invasive bladder cancer heterogeneity by analyzing changes in the biological pathways.

### Materials and methods

**Patients and tissue samples.** This study included a total of 30 patients, derived from 3 risk groups. Thirty samples (cancerous and normal urothelial tissues confirmed by 2 individual pathological diagnoses) were obtained from patients treated at The Affiliated Hospital of Qingdao University immediately after radical cystectomy due to primary invasive bladder cancer (7). The cancerous and the adjacent microscopically normal urothelial (5 cm away) samples were washed 3 times in 5 ml of sterile PBS and then flash frozen in liquid nitrogen within 30 min of removal. Patient consent forms were obtained and tissue-banking procedures were approved by the Institutional Review Board.

**Laser capture microdissection.** Bladder cancer tissue sections were stained with toluidine blue to guide microdissection. Sections (8- $\mu$ m) were air-dried and cut with a Leica AS LMD Laser Capture Microdissection System (Sunnyvale, CA, USA). Approximately 300,000 shoots of tumor or normal urothelial cells from each sample were microdissected and stored on microdissection caps. The cells were captured within 120 min to protect protein from degradation. Cells of interest were dissolved in lysis buffer (65 mM DTT, 4% CHAPS, 95 mM urea, 40% mM Tris). Subsequently, specimens were solubilized via sonication using 20-sec bursts, followed by ice cooling (20 sec), in a process that was repeated 5 times. After completing the above steps, the crude tissue extracts were centrifuged for 45 min at 15,000 rpm to remove the biomembranes, DNA, and other undissolved materials. These tissues were flash frozen in liquid nitrogen and stored at -80°C until use. Fig. 1 shows a representative LCM process of a specimen.

**Sample preparation.** Two hundred micrograms of cancer stromal tissue from 10 cases/group was prepared and digested with trypsin. A total of 100  $\mu$ g of peptides from each group was labeled with iTRAQ reagents following the manufacturer's instructions (Applied Biosystems). Normal group, high risk group, median risk group, and low risk group were labeled with 114, 115, 116 and 117 tags, respectively.

**Strong cation exchange (SCX) separation conditions.** Each set of labeled specimens was dissolved in 10% formic acid and diluted with SCX solvent A (25 mM ammonium formate in 20% acetonitrile, pH 2.8). After that, samples were loaded onto a PolyLC polysulfoethyl A SCX column (2.1-mm internal diameter x 100-mm length, 5  $\mu$ m beads with 300 Å pores). Separation was performed using a linear gradient over 45 min on an ÄKTA purifier system (GE Healthcare, Buckinghamshire, UK). The parameter settings were as follows: flow rate 0.25 ml/min; 0% B (500 mM ammonium formate, pH 2.8, 20% ACN) for 5 min; 0-40% B for 20 min; 40-100% B for 10 min; and 100% B held for 10 min. These fractions were then monitored with UV absorbance detection at 254 and 280 nm and dried by speed vacuuming. The peptide-containing samples were desalted on PepClean C18 spin columns following the manufacturer's protocols (Thermo Fisher Scientific).

**2D LC-MS/MS analysis on LTQ-Orbitrap.** Peptides were dried and resuspended in 0.1% formic acid. LTQ-Orbitrap™ XL (Thermo Fisher Scientific) coupled with a nano-LC system was employed to analyze the samples. The pre-column (75- $\mu$ m internal diameter x 45-mm length) and reversed phase column (50- $\mu$ m internal diameter x 45-mm length) were used to separate peptides. The flow rate for the reversed phase column was 200 nl/min. Each run started from solvent A [(99.9% (v/v) H<sub>2</sub>O, 0.1% (v/v) formic acid)] to 100% solvent B [(15.9% (v/v) H<sub>2</sub>O, 84% (v/v) CH<sub>3</sub>CN and 0.1% (v/v) formic acid)]. The LC eluent was nanosprayed into the LTQ-Orbitrap XL. Collisional-induced dissociation (CID) was used to fragment the precursor peptides and higher-energy collisional-induced dissociation (HCD) was employed to quantify the selected peptides. For LTQ-Orbitrap instruments, data were acquired with the following parameters: MS1 scans and HCD MS2 scans were acquired in Orbitrap with the resolution at 60,000 (m/z 400) and 7500 (m/z 400), respectively; the instrument was operated in a data-dependent mode; 1 microscan for CID-MS2 with collision energy of 30%.

**Database search and protein quantification.** MS data for each fraction were used to identify and quantify proteins based on ProteomicsTools.3.1. (Thermo Fisher Scientific). The database was searched using the Mascot™ search engine. Protein identification was performed at a confidence threshold of 95%. Precursor ion exclusion lists were used to minimize

Table I. Proteins located in the top 10 altered pathways among the three metastatic potential risk groups.

Pathway	SWISS-PROT name in the 3 risk groups		
	Low risk	Median risk	High risk
Systemic lupus erythematosus	ACTN1, ACTN4, <sup>a</sup>	ACTN1, C1S, C7, H2AFY, <sup>a</sup>	C1QC, C1S, C7, <sup>a</sup>
ECM-receptor interaction	CD44, THBS1, <sup>a</sup>	THBS1, <sup>a</sup>	<sup>a</sup>
Amoebiasis	ACTN4, GNAS, ITGAM, <sup>a</sup>	HSPB1, <sup>a</sup>	
Focal adhesion	ACTN1, ACTN4, THBS1, TLN1, <sup>a</sup>	ACTN1, THBS1, TLN1, <sup>a</sup>	GRB2, <sup>a</sup>
Dilated cardiomyopathy (DCM)	GNAS, <sup>a</sup>	<sup>a</sup>	<sup>a</sup>
Hypertrophic cardiomyopathy (HCM)	<sup>a</sup>	<sup>a</sup>	<sup>a</sup>
Complement and coagulation cascades	CD59, PLG, <sup>a</sup>	C1S, C7, CFH, FGA, FGB, FGG, SERPINA1, <sup>a</sup>	C1QC, C1R, C1S, C7, CD59, CFH, FGA, FGB, FGG, PLG, SERPINA1, SERPIND1, <sup>a</sup>
Protein processing in endoplasmic reticulum	DNAJA2, DNAJB11, EIF2S1, SKP1, <sup>a</sup>		CAPN1, ERO1L, HSP90AA1, HSP90AB1, HSP90B1, HYOU1, PDIA3, RPN1, UBQLN1, <sup>a</sup>
Tight junction	<sup>a</sup>		
Parkinson's disease		<sup>a</sup>	
Alzheimer's disease		<sup>a</sup>	
Cardiac muscle contraction		<sup>a</sup>	
Staphylococcus aureus infection			<sup>a</sup>
Proteasome			<sup>a</sup>
Pertussis			<sup>a</sup>
Glutathione metabolism	<sup>a</sup>		

For corresponding pathways, "a" located in Table I represents a set of proteins which are located in Table II.

redundancy. For protein quantification, the ratios of iTRAQ reporter ion intensities from the raw data sets were used to calculate fold changes between samples. The peptides (unique for a given protein) were considered for relative quantitation, excluding those common to other proteins within the same family. The ratios were normalized to the mean value of the 50 ratios identified with the highest number of peptides. Then the protein lists were generated.

**Pathway analysis.** The names of the differentially expressed proteins were converted from IPI database to SWISS-PROT database using Array Track™ (Jefferson, AR, USA) software. Array Track offers a simple query interface to retrieve information concerning human protein expression profile, and provides direct connections to related metabolic and regulatory pathways available from Kyoto Encyclopedia of Genes and Genomes (KEGG) (8). The SWISS-PROT names of the differentially expressed proteins were used for pathway analysis based on Array Track. For statistical analysis, a P-value for

pathway enrichment was obtained using the hypergeometric test, and  $P < 0.05$  was considered to indicate a statistically significant difference.

## Results

**Identification of the differentially expressed proteins.** More than 1,000 proteins were identified and quantified by iTRAQ technique and 2D LC-MS/MS. To obtain the differentially expressed proteins, the protein profiles of different metastatic potential risk groups were compared by paired comparison (high risk vs. median, low risk; median vs. low risk), a total of 3 comparisons. We accepted the differentially expressed proteins as follows: i) proteins reappeared 3 times in the triplicate experiments and ii) proteins were identified based on  $\geq 2$  peptides. Based on these criteria, a total of 1,049 proteins were identified as differentially expressed proteins in our research. In addition, when the protein expression level showed a ratio fold-change  $\geq 1.5$  or  $\leq 0.667$  compared to the normal group

Table II. Commonly expressed proteins in the corresponding pathway.

Pathway	SWISS-PROT name <sup>a</sup>
Systemic lupus erythematosus	C3, C5, C9, HIST1H2BL, HIST1H4A, HIST1H4B, HIST1H4C, HIST1H4D, HIST1H4E, HIST1H4F, HIST1H4H, HIST1H4I, HIST1H4J, HIST1H4K, HIST1H4L, HIST2H4A, HIST2H4B, HIST4H4, HLA-DRB3, SSB
ECM-receptor interaction	COL1A1, COL6A1, COL6A2, COL6A3, DAG1, FN1, LAMA2, LAMA4, LAMA5, LAMC1, TNXB
Amoebiasis	ACTN1, C9, COL1A1, FN1, LAMA2, LAMA4, LAMA5, LAMC1, RAB5C, RAB7A, VCL
Focal adhesion	ACTB, COL1A1, COL6A1, COL6A2, COL6A3, FLNA, FN1, LAMA2, LAMA4, LAMA5, LAMC1, MYL12B, MYL9, PARVA, TNXB, VCL
Dilated cardiomyopathy (DCM)	ACTB, ACTC1, DAG1, DES, LAMA2, LMNA, TPM1, TPM2, TPM3, TPM4
Hypertrophic cardiomyopathy (HCM)	ACTB, ACTC1, DAG1, DES, LAMA2, LMNA, TPM1, TPM2, TPM3, TPM4
Complement and coagulation cascades	A2M, C3, C4BPA, C5, C9, F2, SERPINC1
Protein processing in endoplasmic reticulum	BAG2, BCAP31, CALR, CRYAB, DDOST, UGGT1, ERP29, LMAN1, P4HB, PDIA6
Tight junction	ACTB, ACTN1, ACTN4, CTTN, EXOC4, MYH10, MYH9, MYL12B, MYL9, PPP2CA, RRAS, SPTAN1
Parkinson's disease	ATP5D, ATP5H, COX4I1, COX5B, COX6B1, COX7A2, NDUFA11, NDUFAB1, NDUFV1, SLC25A5, PARK7, SNCA, UQCRC1, VDAC1, VDAC2, VDAC3
Alzheimer's disease	APOE, ATP5D, ATP5H, CALM1, CALM2, CALM3, CHP, COX4I1, COX5B, COX6B1, COX7A2, GAPDH, NDUFA11, NDUFAB1, NDUFV1, SNCA, UQCRC1
Cardiac muscle contraction	ACTC1, COX4I1, COX5B, COX6B1, COX7A2, TPM1, TPM2, TPM3, TPM4, UQCRC1
Staphylococcus aureus infection	C1QC, C1R, C1S, C3, C5, CFH, FGG, HLA-DRB3, KRT10, PLG
Proteasome	PSMA7, PSMB8, PSMC2, PSMC3, PSMC4, PSMD14, PSME3
Pertussis	C1QC, C1R, C1S, C3, C4BPA, C5, CALM1, CALM2, CALM3
Glutathione metabolism	GCLM, GPX3, GSR, GSTM3, IDH1, MGST1, TXNDC12

(high/median/low risk group vs. normal group, respectively, a total of 3 comparisons), we accepted it as a significantly altered protein. After the comparison, 510,549,548 proteins as significantly altered proteins were present in the low/median/high metastatic risk groups, respectively.

**Analysis of the significant pathways.** Differentially expressed proteins (363 of 510) with SWISS-PROT numbers were analyzed by Array Track software (database was accessed on Jun. 12, 2012); similarly 395 of 549 for the median risk group and 388 of 548 for the high risk group. Pathway analysis showed that 198 proteins were located in biological KEGG pathways and were defined as potential biomarkers in the low risk group, and 220/205 proteins in the median/high risk groups, respectively. These proteins were thought to be potential candidate biomarkers for diagnosis or prognosis of bladder cancer. The distinctly altered pathways mainly included focal adhesion, systemic lupus erythematosus and ECM-receptor interaction pathway. Tables I and II show the major altered pathways and the specifically expressed proteins in the different metastatic potential groups.

## Discussion

Bladder cancer is the most common urologic malignant disease, and the features of the mutationally corrupted cells are closely related to the tumorigenic microenvironment (5). Recently, most research concerning bladder cancer has focused on the heterogeneity of the mutated cells, but has neglected the vital role of the stroma which is one of the crucial driving forces for tumor heterogeneity. After protein detection by iTRAQ technique and 2D-LC-MS/MS analysis, 1,049 proteins were identified as being differentially expressed among 3 metastatic risk groups. The smallest and largest molecular weight (MW) values observed in the proteins were 5.5 and 629.1 kDa, and the proteins were distributed across a wide isoelectric point range (3.67-11.98). Several proteins have been reported previously and a significantly altered expression level of these proteins is closely related to tumor characteristics. For example, isocitrate dehydrogenase cytoplasmic enzyme (IDHC) may defend against oxidative damage of cells, and was significantly differentially expressed among the 3 metastatic potential risk groups. Although the

Table III. Top 5 altered pathways in the 3 metastatic potential risk groups.

High risk group	Medium risk group	Low risk group
Complement and coagulation cascades	Systemic lupus erythematosus	Systemic lupus erythematosus
Systemic lupus erythematosus	Complement and coagulation cascades	ECM-receptor interaction
Protein processing in endoplasmic reticulum	Parkinson's disease	Amoebiasis
Staphylococcus aureus infection	ECM-receptor interaction	Focal adhesion
ECM-receptor interaction	Alzheimer's disease	Dilated cardiomyopathy (DCM)

Pathways ranked in ascending order. Results according to P-value.

Table IV. Relative expression levels of various proteins in the 3 metastatic potential risk groups.

Proteins	High/normal	Medium/normal	Low/normal
IDHC	1.43	0.99	0.66
ACTN4	1.27	0.75	0.54
EXOC4	1.21	0.53	0.05
MYH10	0.50	0.21	0.18
ITAM	0.71	1.12	1.66
MMP-9	0.62	1.32	2.21
MIF	1.42	2.86	2.87
FN1	1.57	1.68	2.33
ACTB	0.66	0.52	0.41
A2M	0.35	0.44	0.56
CD44	0.75	0.74	0.45
GRB2	0.62	0.83	0.74

Normal group as baseline.

specific role for the deregulation of IDHC in bladder cancer is not clear, research indicates that the early loss of IDHC may decrease the antioxidant capacity of cells and finally promote tumor progression and metastasis (9).

ACTB ( $\beta$ -actin) is a cytoskeleton structural protein and it regulates motility in several types of cells. In our study, ACTB protein was distinctly weakly expressed in the stroma of muscle-invasive bladder cancer. However, in regards to the intracellular expression level, ACTB was reported to be highly expressed in non-small cell lung cancer cell lines at the mRNA and protein levels. Therefore, the different expression level of ACTB inside and outside cancer cells might be a clue for tumorigenesis (10-12). In our research, the expression level of integrin  $\alpha(M)\beta_2$  (ITAM) increased in turn from the high risk group to the low risk groups (Table IV). Recently, Ma *et al* provided a new insight for ITAM in the aspect of tumor metastatic mechanism. ITAM, a type of immune adhesion molecule, is transferred from innate immune cells to tumor cells via microparticles (derived from innate immune cells). Then the tumor cells acquire a transient immune phenotype and metastasize to distant organs. Due to the protein derived from stromal cells of bladder cancer, the level of ITAM had an inverse relationship between inside the cells and outside

the cells (13). Thus, the different expression levels of ITAM in the 3 metastatic potential risk groups may account for the metastatic potential heterogeneity of bladder cancer.

Multiple altered biological pathways were present in the muscle-invasive bladder cancer and might play a vital role in regulating the metastatic potential heterogeneity of malignant disease. In our study, 510,549,548 proteins were identified as being significantly altered in the low, median and high metastatic potential risk groups, respectively. Two hundred and seventy-one (low risk), 264 (median risk), 208 (high risk) proteins were located in KEGG pathways using Array track software. As shown in Table III, our results illustrated that the divergently altered biological pathways presented in the 3 metastatic potential risk groups may play a key role in regulating the metastatic potential heterogeneity of muscle-invasive bladder cancer. The KEGG pathway of systemic lupus erythematosus (SLE) was one of the significantly altered biological pathways. Immune system dysfunction has been reported to play a vital role in the metastasis of neoplasms (13). Thus, the differentially altered KEGG pathway of SLE among the 3 risk groups (Fig. 3 and Table III) illustrate that immunological dysregulation is one driving force resulting in tumor metastatic potential heterogeneity. The KEGG pathway of SLE was the most prominently altered pathway noted in the list of altered pathways in the low/median metastatic potential risk groups (Table III). There are several types of immunocytes presented on the KEGG SLE pathway map, such as macrophages, neutrophils, antigen-presenting cells.

Macrophage migration inhibitory factor (MIF), upregulated in the 3 metastatic groups (Table IV), is thought to be released from monocytes/macrophages (14) and acts as a regulator of innate immunity. Jung *et al* reported that overexpression of MIF can suppress the tumor-suppressor gene p53, leading to uncontrolled cell growth (15). In addition, overexpression of MIF can result in upregulation of hypoxia inducible factor-1 (HIF-1); this change leads to the overexpression of several genes, such as matrix metalloproteinases (MMPs) and vascular endothelial growth factor (VEGF), consequently promoting tumor metastasis and angiogenesis (16). The differential expression level of MIF among the different risk groups reflects the metastatic potential heterogeneity of muscle-invasive bladder cancer. In the high metastatic potential risk group, the KEGG complement and coagulation cascade pathway was shown as the most prominently altered one (Table III). Nineteen proteins located in this pathway are thought to be candidate biomarkers for bladder cancer

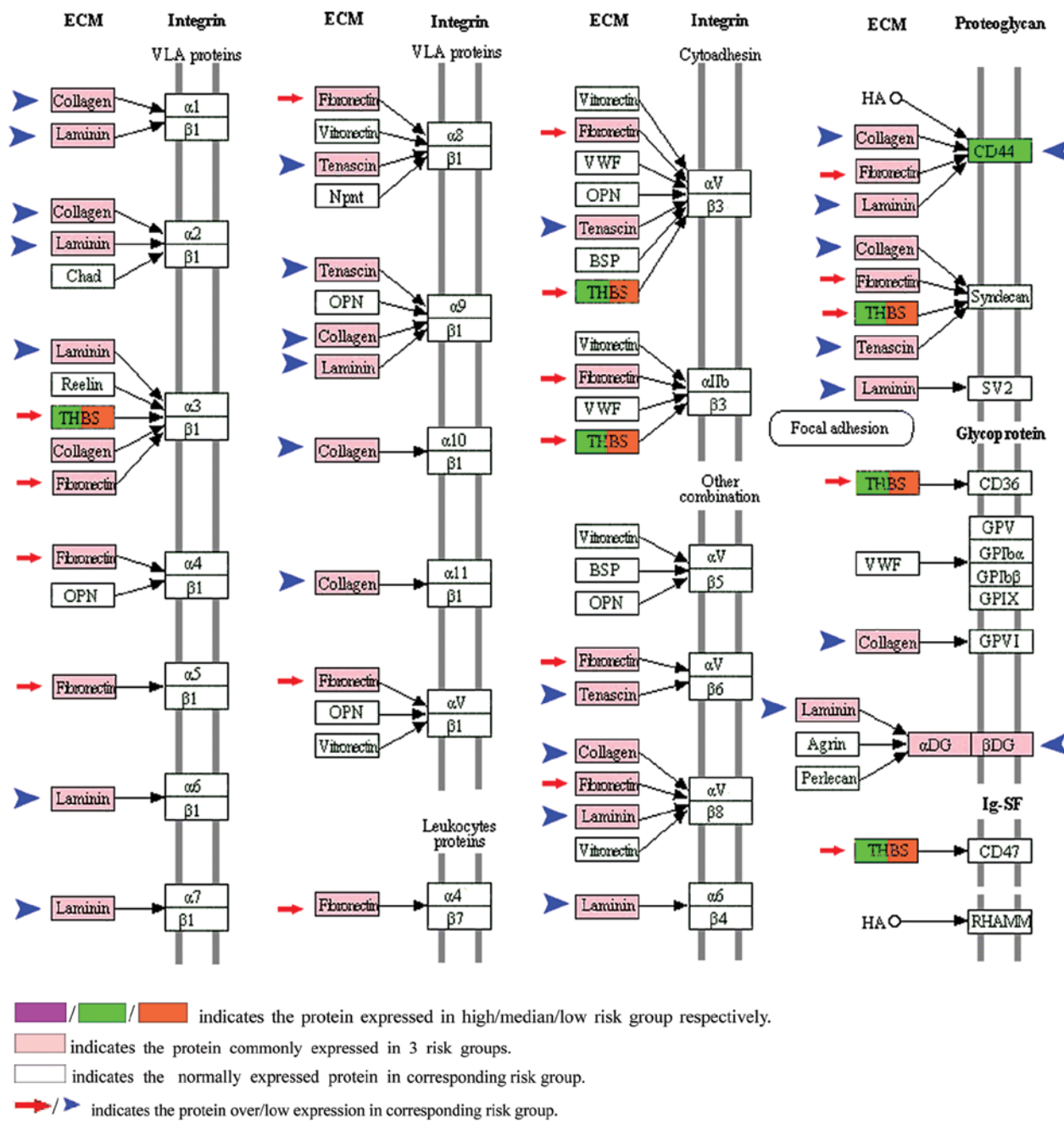


Figure 2. The altered ECM-receptor interaction KEGG pathway among the 3 metastatic risk groups.

(Tables I and II). Among them,  $\alpha$ -2-macroglobulin (A2M) is one of the serum proteinase inhibitors located in this pathway (Table II). Research has shown that the serum level of A2M has an inverse relationship with PSA in prostate cancer patients and A2M (activated state) can promote tumor development and progression by mediating proliferation, pro-migratory, and anti-apoptotic signaling mechanisms (17,18). The other KEGG pathways, including protein processing in endoplasmic reticulum, Staphylococcus aureus infection, ECM-receptor interaction, focal adhesion and tight junction, were also divergently ranked among the 3 metastatic risk groups (Table III). It can be derived from the analysis of the data that the simultaneous change of multi-pathways is one of the effective ways to account for the metastatic potential heterogeneity in terms of muscle-invasive bladder cancer.

To clarify the alterations in pathways, it is necessary to understand the heterogeneity of tumors. In our study, the KEGG ECM-receptor interaction pathway was confirmed as one of the significantly altered pathways among the 3 risk groups. According to the P-value, all altered pathways were ranked in ascending order. The KEGG ECM-receptor interaction pathway ranked 5th in the high risk group, 4th in the median risk group and 2nd in the low risk group, respectively (Table III). Fibronectin (FN1) is a non-collagenous glycoprotein (19) and was upregulated in our results (Table IV). The other proteins, such as collagen, laminin and tenascin were downregulated in the protein list (Fig. 2). All of these proteins were located in the KEGG ECM-receptor interaction pathway. Ioachim *et al* showed that the expression of tenascin, fibronectin and collagen appears to be correlated with more



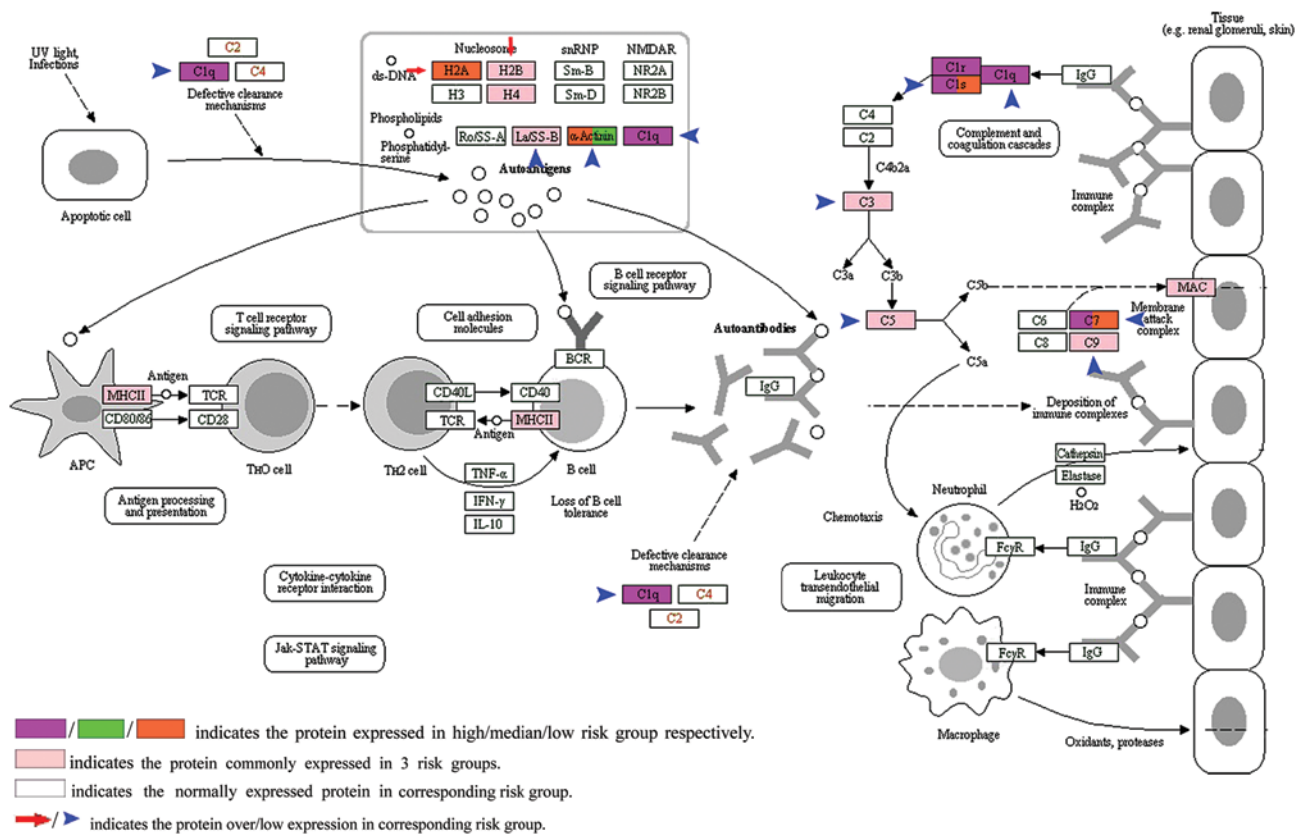


Figure 3. The altered ECM-receptor interaction KEGG pathway among the 3 metastatic risk groups.

aggressive tumor behavior, and their interrelationship could influence tumor progression by remodeling bladder cancer tissue (20). In addition, CD44 was abnormally expressed in the low risk group (Table I). CD44 is a transmembrane glycoprotein which acts as a 'node' to interact with collagen, fibronectin and laminin in the KEGG ECM-receptor interaction pathway (Fig. 2). Henke *et al* indicated that malignant cells used CD44-related chondroitin sulfate proteoglycan as a matrix receptor to mediate metastasis (21). Therefore, the divergently altered KEGG ECM-receptor interaction pathways among the 3 metastatic risk groups reflect that the biological pathways may be pivotal for regulating the metastatic heterogeneity of bladder cancer. Moreover, the KEGG focal adhesion pathway functions as the sub-pathway of the ECM-receptor interaction pathway, and was cross-linked by integrin  $\alpha$  and  $\beta$ , which makes it another significantly altered pathway in our study. According to the P-value, the pathway lists showed that the KEGG focal adhesion pathway ranked 7th in the high risk group and 6th in the median and 4th in the low metastatic risk group. Actinin-4 (ACTN4) and growth factor receptor-bound protein 2 (GRB2) act as candidate biomarkers located in the focal adhesion pathway. ACTN4 was specifically located in the low risk metastatic potential group, and GRB2 in the high risk metastatic potential risk group, respectively. For ACTN4, Yamamoto *et al* indicated that the ACTN4 gene, mapped to the chromosomal band 19q13.1-q13.2, was commonly amplified in ovarian cancer cells. The actinin-4 protein was found to play an important role in the pathogenesis of ovarian cancer (22). In addition, GRB2 acts as a downstream intermediary in several oncogenic signaling pathways. The human GRB2 gene is

located in chromosome 17q22 which is known to be duplicated in solid tumors. GRB2 signaling has been implicated in the pathogenesis of several human cancers (23). Other proteins located in the KEGG focal adhesion pathway were thrombospondin-1 (THBS1) and talin-1 (TLN1) (Tables I and II). From another perspective, mechanical signaling plays a crucial role in the metastasis of tumors. Cells receive mechanical signals from the extracellular matrix through focal adhesions. Focal adhesions are the major sites of interactions between extracellular mechanical signals and intracellular biochemical signaling molecules. Cells respond to signals through integrin-related signaling pathways to maintain cellular migration function. Accordingly, the above analysis provides effective support for the theory which states that biological pathway change may play a crucial role in regulating bladder cancer metastatic heterogeneity (24).

Another contribution of pathway analysis is the confirmation of candidate biomarkers. The protein exocyst complex component 4 (EXOC4) is a key protein in the KEGG tight junction pathway and was expressed differentially among the 3 metastatic risk groups (Table IV). Yamamoto *et al* found that EXOC4 (aliases for EXOC4) was overexpressed in oral squamous-cell carcinoma (OSCC) and plays a crucial role in OSCC progression by promoting secretion of matrix metalloproteinases (MMPs) (25). MMPs can induce gaps in the ECM to promote cancer metastasis by degrading associated proteins (24). The abnormal expression of protein EXOC4 was first identified in muscle-invasive bladder cancer in our study and EXOC4 may act as a candidate biomarker in bladder cancer. In addition, MMP-9 is another protein whose expression level

was significantly altered among the 3 risk groups (Table IV). Some researchers have shown that the MMP gene contained the E2F (E2F is a group of genes that codifies a family of transcription factors) binding site in the promoter region and is regulated by E2F transcription factors which play a crucial role in promoting metastasis (26). Ramón de Fata *et al* found that patients with bladder cancer had a higher level of MMP-9 in the serum than controls, and serum MMP-9 has application in the prediction of the progression of bladder cancer (27). Myosin-10 (MYH10), one of the cytoskeletal regulators, was located in the KEGG tight junction pathway. The expression level is shown in Table IV. MYH10 can regulate mitosis and endothelial cell migration by interacting with microfilaments and microtubules (28). Although little information is available to show the role of myosin-10 in human bladder cancer progression, based on our results, myosin-10 may affect the prognosis of human bladder cancer and is thought to be a candidate biomarker (28,29).

In conclusion, based on our results, 1,049 proteins were identified as being differentially expressed and 510,549,548 proteins as being significantly altered proteins in the low/median/high metastatic risk groups, respectively. Pathway analysis shows that the differentially expressed proteins are mainly located in the systemic lupus erythematosus pathway, ECM-receptor interaction, focal adhesion, and tight junction pathways. Our study confirmed that stroma is an important part of the tumor and plays a vital role in regulating the heterogeneity of muscle-invasive bladder cancer. Commonly altered biological pathways determine the malignant phenotype of muscle-invasive bladder cancer. Biomarker discovery should take into account both neoplastic cells and the corresponding stroma.

## Acknowledgements

This research was supported by a grant from the National Natural Science Foundation of China (nos. 30901481, 81372752, 81101932), the Wu Jieping Medical Foundation (320.6750.13261) and the Doctoral Science Foundation of Shandong Province, China (BS2010YY009).

## References

1. Siegel R, Naishadham D and Jemal A: Cancer Statistics, 2013. *CA Cancer J Clin* 63: 11-30, 2013.
2. Pasin E, Josephson DY, Mitra AP, Cote RJ and Stein JP: Superficial bladder cancer: an update on etiology, molecular development, classification, and natural history. *Rev Urol* 10: 31-43, 2008.
3. Knowles MA: Molecular subtypes of bladder cancer: Jekyll and Hyde or chalk and cheese? *Carcinogenesis* 27: 361-373, 2006.
4. Hasebe T: Tumor-stromal interactions in breast tumor progression - significance of histological heterogeneity of tumor-stromal fibroblasts. *Expert Opin Ther Targets* 17: 449-460, 2013.
5. van der Horst G, Bos L and van der Pluijm G: Epithelial plasticity, cancer stem cells, and the tumor-supportive stroma in bladder carcinoma. *Mol Cancer Res* 10: 995-1009, 2012.
6. De Sousa E Melo F, Vermeulen L, Fessler E and Medema JP: Cancer heterogeneity - a multifaceted view. *EMBO Rep* 14: 686-695, 2013.
7. Niu HT, Shao SX, Zhang ZL, *et al*: Quantitative risk stratification and individual comprehensive therapy for invasive bladder cancers in China: *Int Urol Nephrol* 41: 571-577, 2009.
8. Tong W, Harris S, Cao X, *et al*: Development of public toxicogenomics software for microarray data management and analysis. *Mutat Res* 549: 241-253, 2004.
9. Memon AA, Chang JW, Oh BR and Yoo YJ: Identification of differentially expressed proteins during human urinary bladder cancer progression. *Cancer Detect Prev* 29: 249-255, 2005.
10. Guo C, Liu S, Wang J, Sun MZ and Greenaway FT: ACTB in cancer. *Clin Chim Acta* 417: 39-44, 2013.
11. Andersen CL, Jensen JL and Ørntoft TF: Normalization of real-time quantitative reverse transcription-PCR data: a model-based variance estimation approach to identify genes suited for normalization, applied to bladder and colon cancer data sets. *Cancer Res* 64: 5245-5250, 2004.
12. Saviozzi S, Cordero F, Lo Iacono M, Novello S, Scagliotti GV and Calogero RA: Selection of suitable reference genes for accurate normalization of gene expression profile studies in non-small cell lung cancer. *BMC Cancer* 6: 200, 2006.
13. Ma J, Cai W, Zhang Y, *et al*: Innate immune cell-derived microparticles facilitate hepatocarcinoma metastasis by transferring integrin  $\alpha(M)\beta_2$  to tumor cells. *J Immunol* 191: 3453-3461, 2013.
14. Nishihira J, Ishibashi T, Fukushima T, Sun B, Sato Y and Todo S: Macrophage migration inhibitory factor (MIF): Its potential role in tumor growth and tumor-associated angiogenesis. *Ann NY Acad Sci* 995: 171-172, 2003.
15. Jung H, Seong HA and Ha H: Critical role of cysteine residue 81 of macrophage migration inhibitory factor (MIF) in MIF-induced inhibition of p53 activity. *J Biol Chem* 283: 20383-20396, 2008.
16. Oda S, Oda T, Nishi K, *et al*: Macrophage migration inhibitory factor activates hypoxia-inducible factor in a p53-dependent manner. *PLoS One* 3: e2215, 2008.
17. Kanoh Y, Ohtani H, Egawa S, Baba S and Akahoshi T: Changes of proteases and proteinase inhibitors in androgen-dependent advanced prostate cancer patients with alpha2-macroglobulin deficiency. *Clin Lab* 58: 217-225, 2012.
18. Misra UK, Payne S and Pizzo SV: Ligation of prostate cancer cell surface GRP78 activates a proproliferative and antiapoptotic feedback loop: a role for secreted prostate-specific antigen. *J Biol Chem* 286: 1248-1259, 2011.
19. Brunner A and Tzankov A: The role of structural extracellular matrix proteins in urothelial bladder cancer (review). *Biomark Insights* 2: 418-427, 2007.
20. Ioachim E, Michael M, Stavropoulos NE, Kitsiou E, Salmas M and Malamou-Mitsi V: A clinicopathological study of the expression of extracellular matrix components in urothelial carcinoma. *BJU Int* 95: 655-659, 2005.
21. Henke CA, Roongta U, Mickelson DJ, Knutson JR and McCarthy JB: CD44-related chondroitin sulfate proteoglycan, a cell surface receptor implicated with tumor cell invasion, mediates endothelial cell migration on fibrinogen and invasion into a fibrin matrix. *J Clin Invest* 97: 2541-2552, 1996.
22. Yamamoto S, Tsuda H, Honda K *et al*: ACTN4 gene amplification and actinin-4 protein overexpression drive tumour development and histological progression in a high-grade subset of ovarian clear-cell adenocarcinomas. *Histopathology* 60: 1073-1083, 2012.
23. Giubellino A, Burke TR Jr and Bottaro DP: Grb2 signaling in cell motility and cancer. *Expert Opin Ther Targets* 12: 1021-1033, 2008.
24. Seong J, Wang N and Wang Y: Mechanotransduction at focal adhesions: from physiology to cancer development. *J Cell Mol Med* 17: 597-604, 2013.
25. Yamamoto A, Kasamatsu A, Ishige S, *et al*: Exocyst complex component Sec8: a presumed component in the progression of human oral squamous-cell carcinoma by secretion of matrix metalloproteinases. *J Cancer Res Clin Oncol* 139: 533-542, 2013.
26. Johnson JL, Pillai S, Pernazza D, Sebt SM, Lawrence NJ and Chellappan SP: Regulation of matrix metalloproteinase genes by E2F transcription factors. Rb-Raf-1 interaction as a novel target for metastatic disease: *Cancer Res* 72: 516-526, 2012.
27. Ramón de Fata F, Ferruelo A, Andrés G, Gimbernat H, Sánchez-Chapado M and Angulo JC: The role of matrix metalloproteinase MMP-9 and TIMP-2 tissue inhibitor of metalloproteinases as serum markers of bladder cancer. *Actas Urol Esp* 37: 480-488, 2013.
28. Woolner S, O'Brien LL, Wiese C and Bement WM: Myosin-10 and actin filaments are essential for mitotic spindle function: *J Cell Biol* 182: 77-88, 2008.
29. Ju XD, Guo Y, Wang NN, *et al*: Both Myosin-10 isoforms are required for radial neuronal migration in the developing cerebral cortex. *Cereb Cortex* 24: 1259-1268, 2013.